

Ba₈CoNb₆O₂₄: A spin- $\frac{1}{2}$ triangular-lattice Heisenberg antiferromagnet in the two-dimensional limit

R. Rawl,¹ L. Ge,² H. Agrawal,³ Y. Kamiya,⁴ C. R. Dela Cruz,³ N. P. Butch,⁵ X. F. Sun,^{6,7,8} M. Lee,^{9,10} E. S. Choi,¹⁰ J. Oitmaa,¹¹ C. D. Batista,^{1,12} M. Mourigal,^{2,*} H. D. Zhou,^{1,10,†} and J. Ma^{13,8,1,‡}

¹*Department of Physics and Astronomy, University of Tennessee, Knoxville, Tennessee 37996, USA*

²*School of Physics, Georgia Institute of Technology, Atlanta, Georgia 30332, USA*

³*Quantum Condensed Matter Division, Oak Ridge National Laboratory, Oak Ridge, Tennessee 37381, USA*

⁴*Condensed Matter Theory Laboratory, RIKEN, Wako, Saitama 351-0198, Japan*

⁵*NIST Center for Neutron Research, National Institute of Standards and Technology, Gaithersburg, Maryland 20899, USA*

⁶*Hefei National Laboratory for Physical Sciences at Microscale, University of Science and Technology of China, Hefei, Anhui 230026, People's Republic of China*

⁷*Key Laboratory of Strongly-Coupled Quantum Matter Physics, Chinese Academy of Sciences, Hefei, Anhui 230026, People's Republic of China*

⁸*Collaborative Innovation Center of Advanced Microstructures, Nanjing, Jiangsu 210093, People's Republic of China*

⁹*Department of Physics, Florida State University, Tallahassee, Florida 32306, USA*

¹⁰*National High Magnetic Field Laboratory, Florida State University, Tallahassee, Florida 32310, USA*

¹¹*School of Physics, The University of New South Wales, Sydney, NSW 2052, Australia*

¹²*Quantum Condensed Matter Division and Shull-Wollan Center, Oak Ridge National Laboratory, Oak Ridge, Tennessee 37831, USA*

¹³*Key Laboratory of Artificial Structures and Quantum Control, Department of Physics and Astronomy, Shanghai Jiao Tong University, Shanghai 200240, China*

(Received 3 December 2016; published 17 February 2017)

The perovskite Ba₈CoNb₆O₂₄ comprises equilateral effective spin- $\frac{1}{2}$ Co²⁺ triangular layers separated by six nonmagnetic layers. Susceptibility, specific heat, and neutron scattering measurements combined with high-temperature series expansions and spin-wave calculations confirm that Ba₈CoNb₆O₂₄ is basically a two-dimensional magnet with no detectable spin anisotropy and no long-range magnetic ordering down to 0.06 K. In other words, Ba₈CoNb₆O₂₄ is very close to be a realization of the paradigmatic spin- $\frac{1}{2}$ triangular Heisenberg model, which is not expected to exhibit symmetry breaking at finite temperatures according to the Mermin and Wagner theorem.

DOI: [10.1103/PhysRevB.95.060412](https://doi.org/10.1103/PhysRevB.95.060412)

In a celebrated 1966 paper [1], Mermin and Wagner demonstrated that thermal fluctuations prevent two-dimensional (2D) magnets to spontaneously break their continuous spin-rotation symmetry if the interactions decay fast enough with the distance between spins. The role of thermal fluctuations is replaced by quantum fluctuations in one-dimensional (1D) systems at temperature $T = 0$; for instance, the spin- $\frac{1}{2}$ Heisenberg antiferromagnetic chain does not display long-range magnetic order in the $T = 0$ limit and instead hosts quasi-long-range correlations [2] and fractional spin excitations [3–5]. Quantum fluctuations are also expected to have a strong effect on the ground states of highly frustrated 2D and 3D Mott insulators. Indeed, the realization of *quantum spin liquids*, quantum-entangled states of matter which do not exhibit magnetic ordering, is a major focus of modern condensed matter physics [6,7]. While spin liquids are an extreme case of quantum states of matter, 2D systems that *do* order at $T = 0$ can still exhibit strong deviations from semiclassical behavior. For instance, the elementary excitations of a 2D ordered magnet (magnons) become weakly bonded pairs of fractional excitations near the “quantum melting point” (QMP) that signals the transition into a spin-liquid state. A clear indication of proximity to a QMP is

a strong suppression of the ordered moment relative to the full moment.

The spin- $\frac{1}{2}$ 2D triangular-lattice Heisenberg antiferromagnet (QTLHAF) displays noncollinear spin order at $T = 0$ with a relative suppression of the ordered moment of more than 50% [8–13]. This makes it an ideal model for studying the effect of strong quantum fluctuations on the spectrum of magnetic excitations. In real materials, however, weak interlayer interactions and spin or spatial anisotropies are likely present. Even extremely small perturbations are sufficient to induce long-range magnetic order at a sizable Néel temperature T_N , because T_N increases logarithmically in the interlayer coupling or in the exchange anisotropy [14–18]. This is the case for well-studied compounds comprising transition-metal ions, such as Cs₂CuCl₄ ($T_N = 0.62$ K [19]) and Ba₃CoSb₂O₉ ($T_N = 3.8$ K [20]). Quantum effects remain prominent below T_N and lead to order from disorder phenomena, such as the one-third magnetization plateaus [21–23], in the presence of an external magnetic field. A recent inelastic neutron scattering (NS) study of Ba₃CoSb₂O₉ [24] showed that even in the presence of sizable perturbations [20,25–27] relative to the pure QTLHAF, dynamical features are not captured by spin-wave theory (SWT). This observation suggests that alternative theoretical approaches are not only needed to describe spin-liquid states, but also to account for qualitative properties of the excitation spectrum of ordered magnets near their QMP [28,29].

*mourigal@gatech.edu

†hzhou10@utk.edu

‡jma3@sju.edu.cn

In this Rapid Communication, we introduce $\text{Ba}_8\text{CoNb}_6\text{O}_{24}$, a realization of the QTLHAF model obtained from $\text{Ba}_3\text{CoSb}_2\text{O}_9$ by intercalating nonmagnetic layers between the triangular planes. We present structural, thermomagnetic, inelastic NS, and theoretical results indicating that spin-space anisotropy and interplane interactions are both essentially absent in $\text{Ba}_8\text{CoNb}_6\text{O}_{24}$. Having a model realization of the QTLHAF at hand, we test predictions from semiclassical spin-wave theory and investigate potential exotic phenomena arising from enhanced quantum fluctuations.

To obtain $\text{Ba}_8\text{CoNb}_6\text{O}_{24}$, we start from $\text{Ba}_3\text{CoSb}_2\text{O}_9$, a compound that comprises layers of magnetic CoO_6 octahedral stacked along the hexagonal c axis and separated by two nonmagnetic SbO_6 layers. The intralayer Co-Co distance is 5.86 Å and the interlayer Co-Co distance is 7.23 Å [20]. In the former material, the interlayer magnetic exchange interaction J' is $\sim 5\%$ of the intralayer exchange J [24,26]. Moreover, $\text{Ba}_3\text{CoSb}_2\text{O}_9$ possesses a small easy-plane XXZ anisotropy (the ratio between the longitudinal and transverse exchange interactions is $\Delta \approx 0.9$). While the degree of spin anisotropy is difficult to control, one natural strategy to reduce the interlayer interaction is to insert additional nonmagnetic layers in between the magnetic layers. $\text{Ba}_8\text{CoNb}_6\text{O}_{24}$ exactly meets these requirements: It contains a vacant layer and *six layers* of nonmagnetic NbO_6 octahedral between triangular layers of Co^{2+} ions [see Fig. 1(a)]. While the intralayer Co-Co distance of 5.79 Å is comparable to $\text{Ba}_3\text{CoSb}_2\text{O}_9$, the interlayer Co-Co distance is dramatically increased up to 18.90 Å [30]. This remarkable structure is expected to guarantee a true 2D nature for the magnetic properties of $\text{Ba}_8\text{CoNb}_6\text{O}_{24}$.

To confirm the physical outcome of our intercalation strategy, we present structural and thermomagnetic characterizations of powder samples of $\text{Ba}_8\text{CoNb}_6\text{O}_{24}$ grown from a solid-state synthesis method detailed in the Supplemental Material (SM) [31]. A fit to our neutron powder diffraction (NPD) pattern measured at $T = 0.3$ K with $\lambda = 1.54$ Å [Fig. 1(b)] yields the space group $P\bar{3}m1$ with $a = 5.7902(2)$ Å and $c = 18.9026(3)$ Å. A Rietveld refinement yields structural parameters given in the SM [31] and indicates a limited amount of disorder ($< 2\%$) between the Co and Nb sites, consistent with an earlier study [30]. The patterns at $T = 0.3$ and 2.0 K are essentially identical: No additional Bragg peaks appear and broadening of the existing peaks is not observed within the sensitivity and resolution of our experiment [31], suggesting the absence of a structural transition or long-range magnetic order down to $T = 0.3$ K.

The temperature dependence of the magnetic dc susceptibility $\chi(T)$ shows no sign of magnetic ordering or spin freezing down to $T = 1.8$ K [Fig. 1(c)]. The slope of $1/\chi(T)$ changes around $T = 150$ K; Curie-Weiss fits yield $\mu_{\text{eff}} = 5.01(2)\mu_B$ and $\theta_{\text{CW}} = -25.2(3)$ K for $200 \text{ K} < T < 350 \text{ K}$, and $\mu_{\text{eff}} = 3.89(2)\mu_B$ and $\theta_{\text{CW}} = -4.23(1)$ K for $1.8 \text{ K} < T < 30 \text{ K}$. The effective moment reduction indicates a crossover from a high-spin state ($S = \frac{3}{2}$) to a low-spin state ($S = \frac{1}{2}$) and is typical for Co^{2+} ions in an octahedral environment; see, e.g., ACoB_3 ($A = \text{Cs, Rb}$; $B = \text{Cl, Br}$) [32]. The isothermal dc magnetization at $T = 1.8$ K, shown in Fig. 1(d), indicates that spins saturate above $\mu_0 H_s \approx 4$ T, while a fit to the linear magnetization observed from $\mu_0 H = 5$ to 7 T uncovers a Van Vleck paramagnetic contribution of $0.023\mu_B \text{ T}^{-1}$ per Co^{2+} and

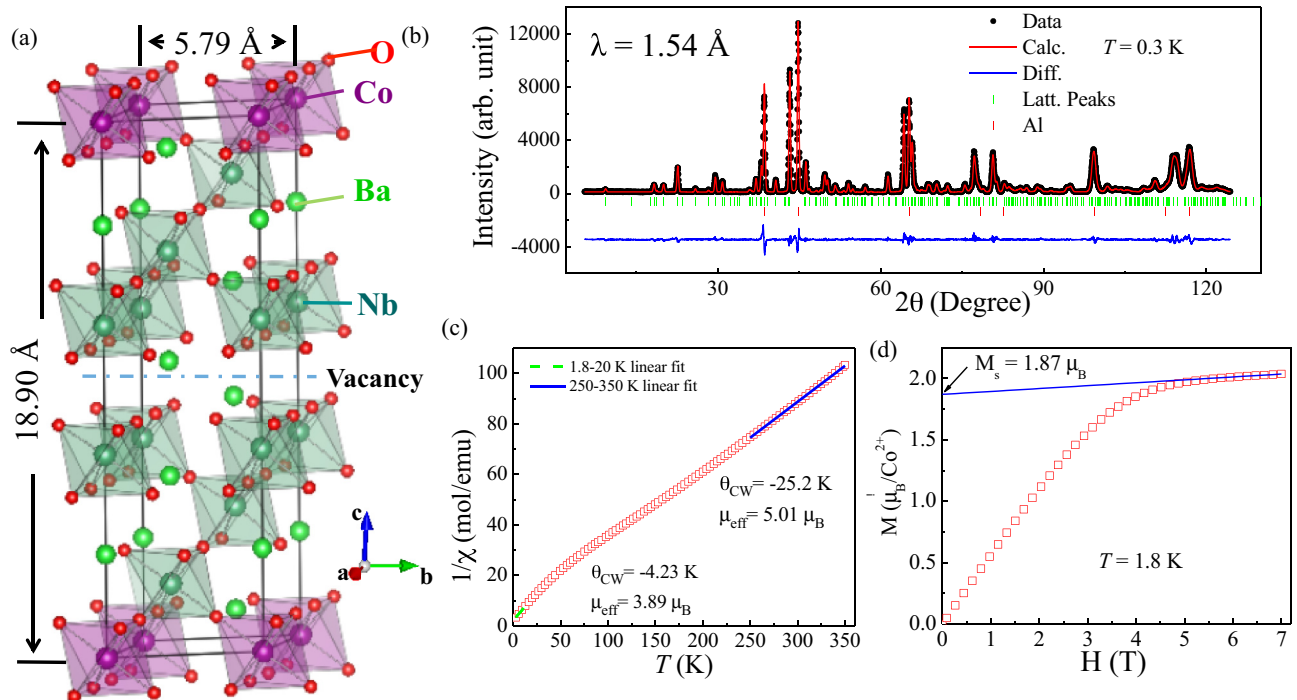


FIG. 1. (a) Stacked layer structure of $\text{Ba}_8\text{CoNb}_6\text{O}_{24}$ with Co^{2+} ions sitting on a triangular lattice. (b) Rietveld refinement of the neutron powder diffraction pattern measured at $T = 0.3$ K with $\lambda = 1.54$ Å. (c) Temperature dependence of the inverse dc magnetic susceptibility and corresponding Curie-Weiss fits. (d) Isothermal dc magnetization measured at $T = 1.8$ K and extrapolation of the saturated magnetization from the linear dependence above the saturation field (blue solid line).

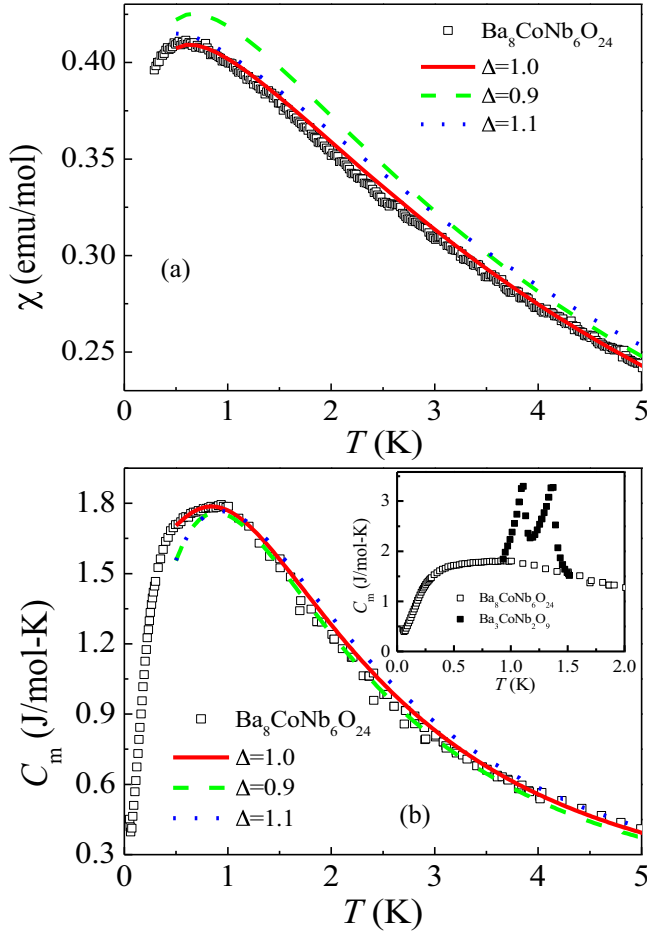


FIG. 2. (a) Temperature dependence of the magnetic ac susceptibility of Ba₈CoNb₆O₂₄ and corresponding high-temperature series expansion simulations for the 2D spin- $\frac{1}{2}$ triangular-lattice antiferromagnet with XXZ exchange anisotropy. Values of $\Delta = 0.9, 1.0,$ and 1.1 are used and simulations run down to a temperature of 0.5 K using Padé approximants of order $[6,6]$. The measurements are obtained with an ac excitation field of amplitude 0.5 Oe and frequency 300 Hz, and matched to the dc susceptibility below $T = 15$ K by an overall T -independent rescaling factor [31]. (b) Temperature dependence of the magnetic part of the specific heat of Ba₈CoNb₆O₂₄ and matching simulations. Inset: Comparison to the magnetic specific heat of Ba₃CoNb₂O₉.

yields a saturation magnetization $M_s = 1.87\mu_B$. This value is comparable to that of Ba₃CoSb₂O₉ and corresponds to a powder-averaged gyromagnetic ratio $g = 3.84$ for the effective $S = \frac{1}{2}$ Kramers doublet.

Similarly, the T dependence of the magnetic ac susceptibility, shown in Fig. 2(a), uncovers no sharp features down to $T = 0.3$ K. Instead, it reveals a broad peak centered at $T = 0.6$ K, which we associate with the onset of short-range magnetic correlations. The presence of magnetic correlations below $T \approx 1$ K is confirmed by the heat-capacity measurements shown in Fig. 2(b). The magnetic contribution to the specific heat C_m was isolated by subtracting the lattice contribution C_L of the isostructural nonmagnetic compound Ba₈ZnTa₆O₂₄ [31]. The $C_m(T)$ curve reveals a broad peak around $T = 0.8$ K without any sharp feature down to $T = 0.06$ K (the small

increase at lower temperatures is attributed to nuclear spins), suggesting the absence of a magnetic phase transition down to $T \leq 0.06$ K. By integrating $C_m(T)/T$ from $T_{\min} = 0.06$ K to a target ($T \leq 8$ K), we obtain the change in magnetic entropy $\Delta S_m = S_m(T) - S_m(T_{\min})$ [31]. The release of entropy reaches 5.32 J mol⁻¹ K⁻¹ at $T = 8$ K, which is close to the value $R \ln 2 = 5.76$ J mol⁻¹ K⁻¹ expected for a Kramers doublet ground state.

What is the origin of the broad peak observed in $C_m(T)$? Previous quantum Monte Carlo studies on quasi-2D antiferromagnetic Heisenberg models have shown that the onset of long-range magnetic order yields a sharp peak in $C_m(T)$ even for interlayer exchange interactions as small as $J'/J = 2 \times 10^{-4}$ [33]. Upon further decreasing the interlayer coupling, the sharp peak disappears and only a broad peak remains. This is precisely the behavior we observe in Ba₈CoNb₆O₂₄, thus exposing the practically ideal 2D nature of magnetism in this compound. This becomes even clearer when our results are compared to Ba₃CoNb₂O₉ [see the inset of Fig. 2(b)], which comprises only two nonmagnetic layers between the magnetic planes. The specific heat of Ba₃CoNb₂O₉ reveals two subsequent phase transitions at $T_{N1} = 1.10$ K and $T_{N2} = 1.36$ K, indicating the presence of easy-axis anisotropy [34]. At a similar energy scale (≈ 1 K), Ba₈CoNb₆O₂₄ only exhibits a single broad peak with no observable signs of exchange anisotropy or interlayer coupling.

The temperature dependence of $\chi(T)$ and $C_m(T)$ for the QTLHAF model has been well documented using high-temperature series expansions (HTSEs) [35–38] up to 12th order [39]. To determine if exchange anisotropy is present in Ba₈CoNb₆O₂₄, we extend existing HTSE work to the XXZ Hamiltonian,

$$\mathcal{H} = J \sum_{\langle i,j \rangle} (S_i^x S_j^x + S_i^y S_j^y + \Delta S_i^z S_j^z), \quad (1)$$

where $\langle i,j \rangle$ denotes nearest-neighbor spins. We obtained results for the isotropic ($\Delta = 1.0$), easy-plane ($\Delta = 0.9$), and easy-axis ($\Delta = 1.1$) models [31]. The best HTSE fit to our experimental observations, namely, $\chi(T)$ and $C_m(T)$ below $T = 5$ K, yields $J = 0.144$ meV for $\Delta = 1.0$ with a fitting error bar on J smaller than 10^{-3} meV (see Fig. 2). For a fixed value of J , the fit quality becomes worse as soon as Δ deviates from 1.0 and leads to higher (respectively lower) peak heights for $\chi(T)$ (respectively C_m).

With a strong thermodynamic indication that Ba₈CoNb₆O₂₄ realizes the purely 2D and spin-isotropic QTLHAF model, we now turn to the nature of its spin excitations. NS intensity (powder averaged) as a function of momentum transfer Q and energy transfer E allows one to track the development of magnetic correlations upon lowering T . In Fig. 3(a), we present such results for $T = 0.3$ K, with additional results for $5 \text{ K} \leq T \leq 0.05$ K included in the SM [31]. The momentum dependence of the magnetic signal reveals strong ridges of intensity emerging from $Q \approx 0.7 \text{ \AA}^{-1}$ with less intense repetitions at 1.5 and 2.0 \AA^{-1} . While spins appear well correlated at $T = 0.3$ K, the low-energy signal ($E \leq 0.1$ meV) remains broader than the instrumental resolution, suggesting that spin correlations remain short ranged and static magnetic order is absent. The energy dependence of the main signal

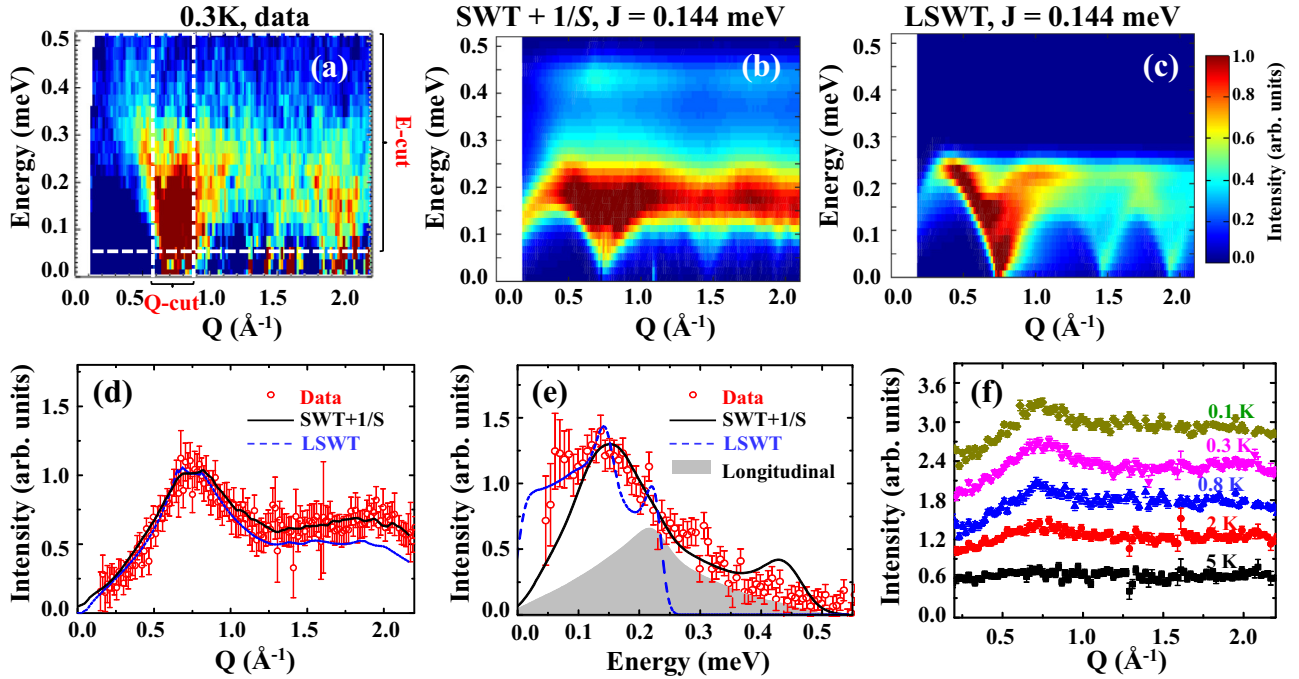


FIG. 3. (a) Powder-averaged inelastic NS spectra of $\text{Ba}_8\text{CoNb}_6\text{O}_{24}$ at $T = 0.3$ K. Data collected at $T = 10$ K are used as the background. (b), (c) NS intensity calculated for $J = 0.144$ meV using nonlinear SWT with $1/S$ corrections and linear SWT, respectively. Calculated intensities have been convoluted by Gaussian profiles of full width at half maximum $\Delta E = 0.025$ meV and $\Delta Q = 0.015$ \AA^{-1} to approximate the effects of instrumental resolution. (d), (e) Comparisons between experiment (red dots), $1/S$ -SWT (solid black line), and linear SWT (dashed blue line) as energy-integrated ($0.05 \leq E \leq 0.52$ meV) and momentum-integrated ($0.6 \leq Q \leq 0.9$ \AA^{-1}) cuts, respectively. The shaded (gray) area corresponds to the longitudinal (two-magnon) contribution to the NS intensity in $1/S$ -SWT. The high-energy bump around $E = 0.45$ meV in (e) is an artifact of our $1/S$ approximation [5]. (f) Temperature dependence of the energy-integrated intensity of (d) and the graphs of different temperatures have been displaced each time by an intensity of 0.6. Error bars correspond to one standard error.

reveals gapless excitations extending up to 0.35 meV with a less intense signal reaching up to $E = 0.45$ meV. These features do not change significantly as T is lower than 0.5 K [31].

To model the dynamic magnetic correlations, we resort to SWT at $T = 0$; $1/S$ corrections [40] are included in Fig. 3(b) while we remain strictly at the linear level (LSWT) [41] in Fig. 3(c). We assume that the system orders in the 120° magnetic structure, at least at $T = 0$, and use $J = 0.144$ meV from the thermodynamic measurements. Our E -integrated [Fig. 3(d)] and Q -integrated [Fig. 3(e)] scans reveal a good agreement between NS measurements and powder-averaged $1/S$ -SWT predictions. The most visible improvement between $1/S$ and linear SWT calculations stems from the inclusion of longitudinal spin fluctuations in the former. These excitations reflect the reduction of the ordered moment by quantum fluctuations and form a high-energy continuum, also known as two-magnon scattering. The absence of a notable temperature dependence for the $E \geq 0.1$ meV magnetic scattering below $T = 0.5$ K [Fig. 3(f)] further supports the evidence for strong quantum fluctuations in the ground state of $\text{Ba}_8\text{CoNb}_6\text{O}_{24}$.

It is instructive to compare the excitations of $\text{Ba}_8\text{CoNb}_6\text{O}_{24}$ with that of the quasi-2D compound $\text{Ba}_3\text{CoSb}_2\text{O}_9$, for which $J' = 0.05J$, $J \approx 1.7$ meV, and $\Delta \approx 0.9$. While both compounds comprise structurally similar magnetic layers with comparable Co-Co bond lengths, the ~ 2.0 meV in-plane excitation bandwidth of $\text{Ba}_3\text{CoSb}_2\text{O}_9$ is an order of

magnitude larger than the present observation of ~ 0.18 meV for $\text{Ba}_8\text{CoNb}_6\text{O}_{24}$. In units of their respective J , the bandwidth $W \approx 1.18J$ for the former compound compares well with $W \approx 1.24J$ obtained by the present $1/S$ -SWT analysis for $\text{Ba}_8\text{CoNb}_6\text{O}_{24}$ [see Fig. 3(b)]. While $\text{Ba}_3\text{CoSb}_2\text{O}_9$ develops long-range magnetic ordering below $T_N = 3.7$ K $\sim 0.19J$, $\text{Ba}_8\text{CoNb}_6\text{O}_{24}$ does not exhibit any magnetic ordering down to $T = 0.06$ K $\sim 0.04J$. Given that T_N increases logarithmically both in the magnitude of J' and Δ , the suppression of T_N/J by a factor of at least 4 relative to $\text{Ba}_3\text{CoSb}_2\text{O}_9$ implies that interplane and anisotropic exchange interactions must be extremely small in $\text{Ba}_8\text{CoNb}_6\text{O}_{24}$.

In conclusion, our powder-sample experiments reveal that $\text{Ba}_8\text{CoNb}_6\text{O}_{24}$ is virtually an ideal realization of the QTLHAF and a unique compound to expose the consequences of the Mermin and Wagner theorem in a real triangular-lattice material. Recent studies have shown that quantum fluctuations have a nonperturbative effect on the magnetic excitations of quasi-2D quantum antiferromagnets [24,42]. We expect even stronger quantum effects in the magnetic excitation spectrum of $\text{Ba}_8\text{CoNb}_6\text{O}_{24}$, making it an even better candidate to challenge existing semiclassical theories for the dynamic response of frustrated quantum antiferromagnets. From the materials discovery standpoint, our work devises a method for reducing dimensionality by intercalating nonmagnetic layers in layered compounds that can be extended to other lattices to reveal different physics.

J.M. thanks the support of the Ministry of Science and Technology of China (2016YFA0300500). R.R. and H.D.Z. thank the support of NSF-DMR-1350002. The work at Georgia Tech (L.G., M.M.) was supported by the College of Sciences and ORAU's Ralph E. Powe Junior Faculty Enhancement Award. Y.K. acknowledges support by JSPS Grants-in-Aid for Scientific Research under Grant No. JP16H02206. X.F.S. acknowledges support from the National Natural Science Foundation of China (Grants No. 11374277 and No.

U1532147), the National Basic Research Program of China (Grants No. 2015CB921201 and No. 2016YFA0300103), and the Opening Project of Wuhan National High Magnetic Field Center (Grant No. 2015KF21). The work at NHMFL is supported by NSF-DMR-1157490, the State of Florida, and the U.S. Department of Energy. The work at ORNL High Flux Isotope Reactor was sponsored by the Scientific User Facilities Division, Office of Basic Energy Sciences, U.S. Department of Energy.

-
- [1] N. D. Mermin and H. Wagner, *Phys. Rev. Lett.* **17**, 1133 (1966).
- [2] E. Lieb, T. Schultz, and D. Mattis, *Ann. Phys.* **16**, 407 (1961).
- [3] L. D. Faddeev and L. A. Takhtajan, *Phys. Lett. A* **85**, 375 (1981).
- [4] D. A. Tennant, T. G. Perring, R. A. Cowley, and S. E. Nagler, *Phys. Rev. Lett.* **70**, 4003 (1993).
- [5] M. Mourigal, M. Enderle, A. Klöpperpieper, J.-S. Caux, A. Stunault, and H. M. Rønnow, *Nat. Phys.* **9**, 435 (2013).
- [6] L. Savary and L. Balents, *Rep. Prog. Phys.* **80**, 016502 (2017).
- [7] A. Banerjee, C. A. Bridges, J.-Q. Yan, A. A. Aczel, L. Li, M. B. Stone, G. E. Granroth, M. D. Lumsden, Y. Yiu, J. Knolle, S. Bhattacharjee, D. L. Kovrizhin, R. Moessner, D. A. Tennant, D. G. Mandrus, and S. E. Nagler, *Nat. Mater.* **15**, 733 (2016).
- [8] Th. Jolicoeur and J. C. Le Guillou, *Phys. Rev. B* **40**, 2727 (1989).
- [9] A. V. Chubukov, S. Sachdev, and T. Senthil, *J. Phys.: Condens. Matter* **6**, 8891 (1994).
- [10] L. Capriotti, A. E. Trumper, and S. Sorella, *Phys. Rev. Lett.* **82**, 3899 (1999).
- [11] W. H. Zheng, J. O. Fjærestad, R. R. P. Singh, R. H. McKenzie, and R. Coldea, *Phys. Rev. B* **74**, 224420 (2006).
- [12] S. R. White and A. L. Chernyshev, *Phys. Rev. Lett.* **99**, 127004 (2007).
- [13] A. L. Chernyshev and M. E. Zhitomirsky, *Phys. Rev. B* **79**, 144416 (2009).
- [14] K. Hirakawa, *J. Appl. Phys.* **53**, 1893 (1982).
- [15] A. Cuccoli, T. Roscilde, R. Vaia, and P. Verrucchi, *Phys. Rev. Lett.* **90**, 167205 (2003).
- [16] S. Miyashita and H. Kawamura, *J. Phys. Soc. Jpn.* **54**, 3385 (1985).
- [17] W. Stephan and B. W. Southern, *Phys. Rev. B* **61**, 11514 (2000).
- [18] S. Fujimoto, *Phys. Rev. B* **73**, 184401 (2006).
- [19] R. Coldea, D. A. Tennant, R. A. Cowley, D. F. McMorrow, B. Dorner, and Z. Tylczynski, *Phys. Rev. Lett.* **79**, 151 (1997).
- [20] Y. Doi, Y. Hinatsu, and K. Ohoyama, *J. Phys.: Condens. Matter* **16**, 8923 (2004).
- [21] H. Tsujii, C. R. Rotundu, T. Ono, H. Tanaka, B. Andraka, K. Ingersent, and Y. Takano, *Phys. Rev. B* **76**, 060406 (2007).
- [22] W.-J. Hu, S.-S. Gong, W. Zhu, and D. N. Sheng, *Phys. Rev. B* **92**, 140403 (2015).
- [23] G. Koutroulakis, T. Zhou, Y. Kamiya, J. D. Thompson, H. D. Zhou, C. D. Batista, and S. E. Brown, *Phys. Rev. B* **91**, 024410 (2015).
- [24] J. Ma, Y. Kamiya, T. Hong, H. B. Cao, G. Ehlers, W. Tian, C. D. Batista, Z. L. Dun, H. D. Zhou, and M. Matsuda, *Phys. Rev. Lett.* **116**, 087201 (2016).
- [25] Y. Shirata, H. Tanaka, A. Matsuo, and K. Kindo, *Phys. Rev. Lett.* **108**, 057205 (2012).
- [26] T. Susuki, N. Kurita, T. Tanaka, H. Nojiri, A. Matsuo, K. Kindo, and H. Tanaka, *Phys. Rev. Lett.* **110**, 267201 (2013).
- [27] N. A. Fortune, S. T. Hannahs, Y. Yoshida, T. E. Sherline, T. Ono, H. Tanaka, and Y. Takano, *Phys. Rev. Lett.* **102**, 257201 (2009).
- [28] H. D. Zhou, C. Xu, A. M. Hallas, H. J. Silverstein, C. R. Wiebe, I. Umegaki, J. Q. Yan, T. P. Murphy, J.-H. Park, Y. Qiu, J. R. D. Copley, J. S. Gardner, and Y. Takano, *Phys. Rev. Lett.* **109**, 267206 (2012).
- [29] E. A. Ghioldi, A. Mezio, L. O. Manuel, R. R. P. Singh, J. Oitmaa, and A. E. Trumper, *Phys. Rev. B* **91**, 134423 (2015).
- [30] P. M. Mallinson, M. M. Allix, J. B. Claridge, R. M. Ibberson, D. M. Iddles, T. Price, and M. J. Rosseinsky, *Angew. Chem Int. Ed.* **44**, 7733 (2005).
- [31] See Supplemental Material at <http://link.aps.org/supplemental/10.1103/PhysRevB.95.060412> for more details on neutron powder diffraction, magnetic susceptibility, specific heat, inelastic neutron scattering, and spin-wave theory.
- [32] M. F. Collins and O. A. Petrenko, *Can. J. Phys.* **75**, 605 (1997).
- [33] P. Sengupta, A. W. Sandvik, and R. R. P. Singh, *Phys. Rev. B* **68**, 094423 (2003).
- [34] M. Lee, J. Hwang, E. S. Choi, J. Ma, C. R. Dela Cruz, M. Zhu, X. Ke, Z. L. Dun, and H. D. Zhou, *Phys. Rev. B* **89**, 104420 (2014).
- [35] N. Chandrasekharan and S. Vasudevan, *Phys. Rev. B* **54**, 14903 (1996).
- [36] H. Rosner, R. R. P. Singh, W. H. Zheng, J. Oitmaa, and W. E. Pickett, *Phys. Rev. B* **67**, 014416 (2003).
- [37] R. R. P. Singh and J. Oitmaa, *Phys. Rev. B* **85**, 104406 (2012).
- [38] J. Oitmaa, C. Hamer, and W. Zheng, *Series Expansion Methods for Strongly Interacting Lattice Models* (Cambridge University Press, Cambridge, U.K., 2006).
- [39] N. Elstner, R. R. P. Singh, and A. P. Young, *Phys. Rev. Lett.* **71**, 1629 (1993).
- [40] M. Mourigal, W. T. Fuhrman, A. L. Chernyshev, and M. E. Zhitomirsky, *Phys. Rev. B* **88**, 094407 (2013).
- [41] S. Toth and B. Lake, *J. Phys.: Condens. Matter* **27**, 166002 (2015).
- [42] B. Dalla Piazza, M. Mourigal, N. B. Christensen, G. J. Nilsen, P. Tregenna-Piggott, T. G. Perring, M. Enderle, D. F. McMorrow, D. A. Ivanov, and H. M. Rønnow, *Nat. Phys.* **11**, 62 (2015).